Proceedings of 14th IOE Graduate Conference
Peer Reviewed
Year: 2023 Month: December Volume: 14
ISSN: 2350-8914 (Online), 2350-8906 (Print)

Temperature Analysis of Electric Vehicle Lithium-Ion Cell

Anuska Gautam [a], Ajay Kumar Jha [b]

[a] *Department of Mechanical and Aerospace Engineering, Pulchowk Campus, IOE, Tribhuvan University, Nepal*
[a] anuskagautam4@gmail.com, [b] akjha@ioe.edu.np

Abstract

A lot of research has been done on the constant discharge process of lithium-ion batteries, but studies on the thermal behavior of lithium-ion batteries during operation under realistic cycles are scarce. So, the main aim of this study was to better understand the temperature variation of a lithium-ion battery cell when it is charging/discharging. For this study, the thermal responses of a lithium-ion cell will be carried out in ANSYS and compared. To accomplish this, each cell was subjected to several discharge and charging processes. The result obtained was in the form of temperature contours and plots evaluating which the thermal response of the cell was compared. In ANSYS, first, a cell was simulated with a series of simple discharges at different C-rates. Next, a combined cycle with a few alternating charge/discharge processes will be prepared, and the changes in the temperature, total heat, and voltage will be observed. The simulations were done for various constant discharge rates. An evaluation of the result from discharge according to discharge rates ranging from 0.3 C, 1C and 3 C for environmental temperature of 300K was done. Then the cells and module were simulated by employing different cooling fluids. The change in maximum temperature was observed and the appropriate coolant was selected. A sample test to observe the temperature increase in cells during discharging was performed for 0.3 C and its results were noted. For simple discharge, 3M Novec 7100 is found to be a better cooling fluid. While for charge-discharge cycles, water was found to be a better coolant.

Keywords

Electric Vehicle, Lithium-ion battery, discharge rate

1. Introduction

1.1 Background

Electric Vehicles (EVs) are at the heart of our time's industrial revolution, where enormous resources and efforts are being poured into advancing toward zero CO_2 emissions to minimize global warming and save the world. The lithium-ion battery (LIB) is a preferred power source for hybrid electric vehicles (HEVs) and electric vehicles (EVs) due to its high energy density, high voltage, and low self-discharge rate. The characteristics of Lithium batteries have made them attractive for automotive applications.

However, despite its attractive prospect, Li-ion battery-based EVs have not been widely adopted by consumers. The major hindrances regarding the battery system include the high cost, limited calendar life, safety concerns, and temperature-caused issues[1]. Temperature has a large effect on the safety, lifetime and performance of Li-ion batteries. To maintain its optimal performance, a narrow temperature range between 15 °C and 35 °C is recommended [2]. Temperatures outside the desired range will result in significant capacity loss. The increment of working temperature in the temperature range of 30–40 °C decreases the calendar life of the battery immensely [3]. It is worth noting that when the cell temperature exceeds the threshold thermal runaway will be triggered which may in turn lead to a terrible catastrophe [4]. In addition, the maximum temperature difference among cells and modules in the battery pack is desired to be less than 5 °C [5].

Battery thermal management systems (BTMS) are designed to regulate the temperature of lithium-ion batteries in electric vehicles (EVs) and other applications. A BTMS is typically made up of several components, including a thermal management controller, sensors, and cooling or heating elements. BTMS use several thermal management techniques and coolants, such as air-cooling, liquid cooling and phase change materials (PCM)[6]. Liquid coolants are generally deemed more efficient than the other two options, due to their higher thermal conductivity than air and PCM [7].

2. Literature Review

The foremost concern while developing electric vehicles is safety, and it is essential to incorporate an efficient BTMS in Li-ion based EVs, HEVs, and PHEVs to quickly dissipate the heat generated within the battery pack. Diagnostic methods that are effective for Li-ion batteries are crucial to ensure that they function within the specified voltage and temperature range to prevent untimely deterioration and breakdown [8]. When lithium-ion batteries are charged or discharged, they produce heat which is mainly transferred from the internal part to the surface of the battery and then dissipated into the environment by means of an effective thermal management system such as ambient air or other coolants. The remaining energy is stored within the battery. Therefore, creating thermal models of batteries involves selecting appropriate equations, such as those for energy balance, heat generation, and boundary conditions [9].

Another study explores the thermal performance of a lithium-ion battery module that powers an electric vehicle, specifically for the WLTP Class 2 test procedure. The simulation was carried out for three different cooling rate profiles based on the driving cycle characteristics, with low, moderate, and high-speed sub-parts. The thermal behavior of the module was evaluated by analyzing the temperature gradients and reference points on the cell wall located near the maximum and minimum temperatures [10]. In this study, the authors investigate the feasibility of using numerical simulation to predict temperature changes during discharge of a li-ion battery. They developed a numerical model using SolidWorks and ANSYS Fluent software and compared the results to real measurements obtained through electrical impedance spectroscopy and thermal imaging. The authors found that the MSMD numerical model provided relatively high accuracy results with a fast calculation speed of a few minutes. However, the computational mesh quality greatly affected the computational time and accuracy, with finer and higher-quality meshes leading to more accurate results [11].

2.1 Models of Battery Simulation in ANSYS

The Ansys/Fluent platform will be used to simulate the electro-thermal cell. For this the well-known Fluent Multi-Scale Multi-Domain (MSMD) technique aids in coping with various physics in solution domains (anode-separator-cathode layers). When this method of modeling is used, the battery electrical and thermal fields are solved in the CFD domain at the scale of the battery cell using the differential equations:

$$\frac{\delta_p . C_p . T}{\delta T} - \nabla.(k \nabla T) = \sigma_+ \left| \nabla \phi_+ \right|^2 + \sigma_- \left| \nabla \phi_- \right|^2 + \dot{q}_{ECh} + \dot{q}_{short} \quad (1)$$

$$\nabla.(\sigma_+ \nabla \phi_+) = -(j_{ECh} - j_{short}) \quad (2)$$

$$\nabla.(\sigma_- \nabla \phi_-) = (j_{ECh} - j_{short}) \quad (3)$$

where σ_+ and σ_- are the effective electric conductivities for the positive and negative electrodes, ϕ_+ and ϕ_- are phase potentials for the positive and negative electrodes j_{ECh} and $\dot{q}_{ECh}$ are the volumetric current transfer rate and the electrochemical reaction heat due to electrochemical reactions, respectively; j_{short} and $\dot{q}_{short}$ are the current transfer rate and heat generation rate due to battery internal short-circuit, respectively; in this case not needed.

2.1.1 NTGK model

The thermal and electrochemical model of the battery module was created with the Newman, Tiedemann, Gu and Kim (NTGK) model [21] proposed by Kwon et al. [22] and validated by others. Volumetric current transfer rate J (A/m3), which are important parameter used in this model, is calculated by the algebraic equation as given below.

$$j_{Ech} = a \times [U - (\phi_+ - \phi_-)] \quad (4)$$

where a is the specific area of the electrode sheet, U and Y are functions of depth of discharge (DOD) and obtained by fitting voltage-current response curves from experiments or provided by the manufacturer. ϕ_+ and ϕ_- denote phase potentials (V) for the negative and positive electrodes. The electrochemical reaction heat, which is an important parameter in our study and affects the temperature increase of the battery module, is calculated as follows:

$$\dot{q}_{Ech} = J_{Ech} \times (V_{oc} - V) - J_{Ech} \times T \times \frac{dV}{dT} \quad (5)$$

where, $\dot{q}_{Ech}$ is the electrochemical reaction heat (W/m3), J_{Ech} is the volumetric charge or discharge current transfer rate (A/m3), V and $V_o c$ represent cell voltage and open circuit voltage (V) respectively, T is also the temperature in K. In Equation 5, the first term is due to ohmic losses and is known as over potential. Since the entropic heat coefficient is obtained by using the derivative of the potential with respect to the temperature, the second term in Equation 2 is called entropic heat.

2.2 Types of Battery Configuration used in Electric Vehicles

The battery system integrates multiple cells and other control circuits into a single battery to power the EV. An electric vehicle's (EV) battery configuration refers to the arrangement of individual battery cells within the battery pack. The battery configuration can affect the capacity, voltage, capacity, and the overall performance of it. For EV batteries, the most common configuration is a series-parallel hybrid design. other cells are connected in series to raise the voltage of the battery pack, and other groups of series-connected cells are then connected in parallel to raise the overall capacity of the battery pack. The series connection of cells raises the voltage output of the battery pack, which is required to provide the required power output to run the vehicle. The parallel connecting of cell groups enhances the capacity of the battery pack, which is necessary for storing the energy needed to drive the automobile to a specific range. The battery design utilized in an EV is affected by a number of criteria, including the required power output, range, and overall vehicle weight [12].

3. Research Methodology

The conceptual framework of this study is shown in figure 1 and its various elements are discussed in the paper.

4. Description of the Study

The simulation is done using two different approaches, first is discharge at constant C-rates, and another is charge and discharge using a combined cycle.

4.1 Simple discharge response

First, a series of basic processes for discharge will be carried out. Three discharges with varying C-rates will be simulated for each model: one at 0.3 C, another at 1 C, and a final one at 3 C. The C-rate is a measure of how quickly a battery charges or discharges, and it can be described as the ratio of current through the battery to the theoretical current at which the battery would supply its nominal capacity in one hour. The nominal capacity of the battery chosen is 50 Ah, which means that a current of 50 A corresponds to a C-rate of 1 C and will deplete the battery in 1 hour.

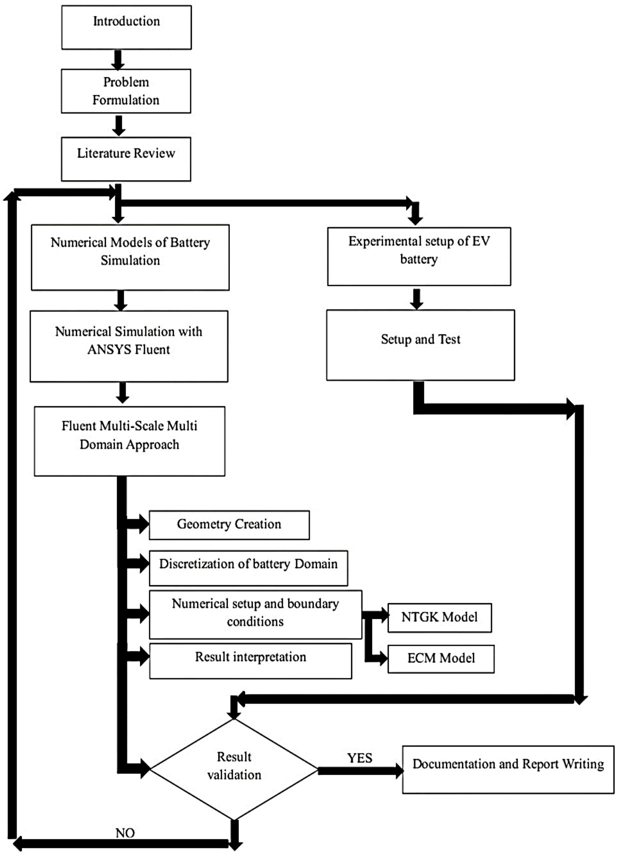

Figure 1: Methodology

- Temperature: This is a critical variable in electric batteries in general, and in Li-ion batteries in particular, since if the temperature decreases, the battery's discharge capacity declines, and if it increases too rapidly, thermal runaway develops, culminating in the cell's catastrophic breakdown.
- Heat source: The total quantity of heat produced by the battery. Joule heat (due to the Joule effect generated by the flow of electrons through the battery, also known as irreversible heat), Electrochemical heat (also known as reversible heat), and short-circuit heat are the three forms of heat.
- Passive zone potential: the difference in potential between the batteries's positive and negative terminals. It normally decreases with increasing SOC and increases with increasing temperature.

4.2 Compound cycle response

The behavior of each cell/module in the presence of rapid changes in electrical load will be studied as the second phase of the study. To do this, a compound cycle comprised of numerous alternating charge and discharge cycles will be prepared, with the goal of substantially simulating the behavior of a battery in an electric or hybrid car, followed by a stable charging process. The cycle, which is designed as a function of flow time, uses current intensities, C-rates, and powers to calculate charge and discharge rates. It is broken into 9 segments and has a total simulation time of 900 seconds. The cycle has the following elements:

1. Discharging at 200 W for 150 s
2. Charging at 1 C for 40 s
3. Discharging at 1 C for 60 s
4. Charging at 5 A for 60 s
5. Discharging at 5 C for 20 s
6. Discharging at 0.5 C for 100 s
7. Discharging at 100 W for 30 s
8. Discharging at 400 W for 40 s
9. Charging at 1 C for 400 s

5. ANSYS Setup

5.1 Geometry

A 50 Ah LIB comprising of $LiFePO_4$ cathode was modeled for this work. The dimensions of the cell are: For active zone: 185mm×160 mm×36mm For tab zones: 35mm×28mm×7mm

To create the geometry, we will use the ANSYS DesignModeler tool.

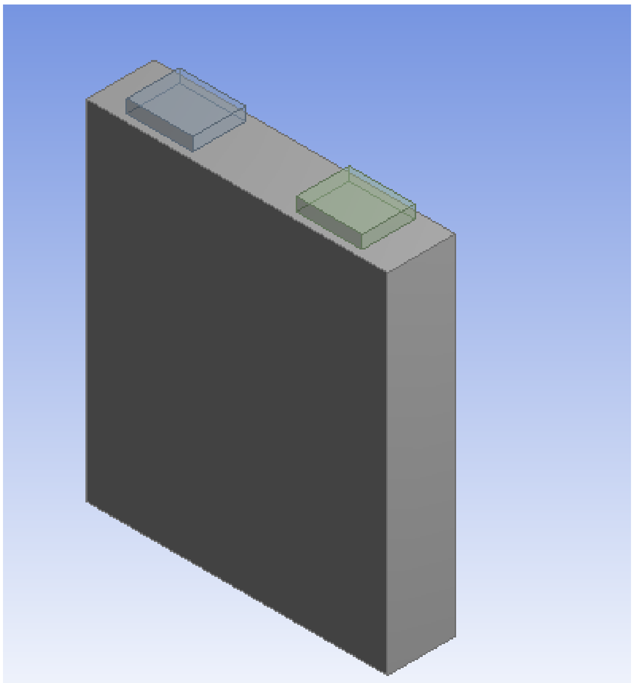

Figure 2: Geometry of single cell

5.2 Meshing

The Meshing tool of ANSYS will be used to mesh our domain. For simplification, meshing with a linear element with a size of 0.002m is done. The total number of elements for the single cell of highstar is 135936 and a representation of the mesh can be seen in Figure 2.

5.3 Setup

Now that the mesh has been completed and imported into FLUENT, the required conditions are applied to the model. This will be done in accordance with the ANSYS Fluent Tutorial Guide's guidelines. The next step is to add-on the Dual-Potential MSMD battery model to ANSYS Fluent, and enable the energy equation and transient state. After this, the

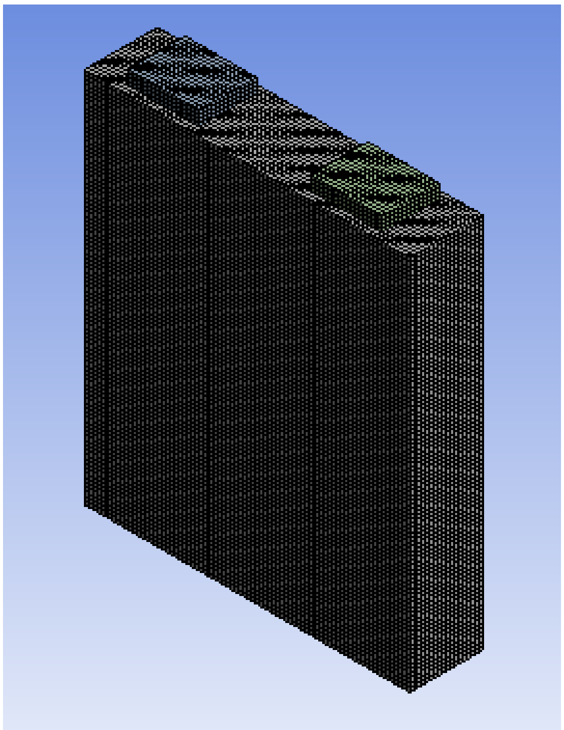

Figure 3: Meshed domain

battery model options are defined. Then NTGK parameters are selected for simulation (which is provided default by ANSYS as seen in figure 9). The simulation is done using two different approaches, first is discharge at constant C-rates, and another is charge and discharge using a combined cycle.

5.3.1 Simple Discharge

The nominal cell capacity for Highstar cell is 50Ah, and the C-rate will be set. For a simple discharge process, this C-rate will remain constant during the simulation. In the conductive zone window, the cell zone is selected at the active component, while the remaining zones: busbar, tabs zones are selected as passive zone. Finally in the electric contact window, the two tabs are specified where ptab represents the positive tab of the cell and ntab represents the negative tab. After this, the battery configuration is checked in this MSMD add-on. After it prints the battery configuration as ok, the battery model is fully defined and now the materials will be covered.

Table 1: Material Properties

Properties	Aluminium	Copper	LIB Cell material
Density (kg/m^3)	2719	8978	2098
Electrical conductivity (s/m)	3.541×10^7	5.8×10^7	5.8×10^7
Thermal Conductivity (W/m.k)	202.4	387.6	18.2
Specific Heat (J/kg.K)	871	381	678

To determine which coolant had the optimum cooling performance in BTMS, three types of coolant were examined and evaluated. Along with the water cooling, two conventional coolants—air and 3M Novec 7100—were also simulated.

Table 2: Coolant Properties

Coolant	Air	Water	3M Novec-7100
Density (kg/m^3)	1.225	998.2	1510
Viscosity (kg/m.s)	1.79×10^{-5}	0.001003	6×10^{-4}
Thermal Conductivity (W/m.k)	0.025	0.6	0.069
Specific Heat (J/kg.K)	1006.43	4182	1183

5.3.2 Compound cycle

The proper way to input the combination/ compound cycle to ANSYS is by describing its various components into a txt file. Fluent supports two different types of profile for these kind of simulations. The first is a timed scheduled profile where with flow time the value of the electric load changes. The next profile is an event-scheduled profile where there is a forwarding condition to change from one load to the next. The way these profiles are presented is also different on the basis of no. of columns. The time scheduled profile has 3 columns in its .txt file while the event scheduled profile has 4 columns.

6. Results and Discussion

6.1 For single cell

6.1.1 For single cell under different discharge rates:

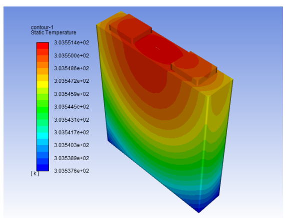

(a) At 0.3 C discharge

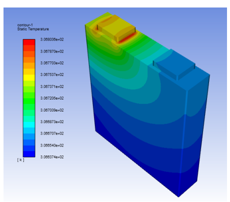

(b) At 1C discharge

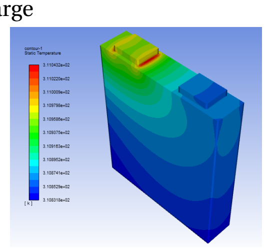

(c) At 3C discharge

Figure 4: Temperature contours for single cell

It was seen that with increase in C rate the temperature of the cell increased drastically. The maximum temperature of

303.551 K, 306.8 K, 311.04 K was seen for cells when simulated with 0.3C, 1C and 3C rate respectively. Whereas for 3C, temperature reached maximum pretty soon. It can be seen that temperature homegenity across the cell was affected by increasing the discharge rate.

6.1.2 For single cell (air cooled) under different discharge rates:

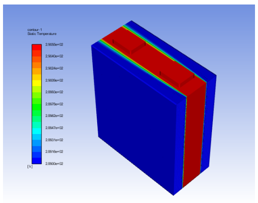

(a) At 0.3 C rate

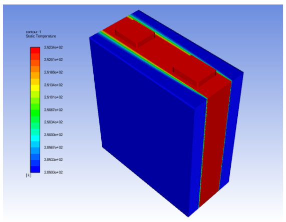

(b) At 1 C rate

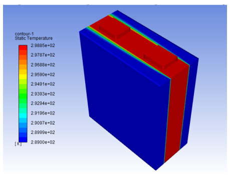

(c) At 3 C rate

Figure 5: Temperature contours for air cooled cell

It was observed that the effect of increasing C rate on the cell increased the temperature.The maximum temperature of 290.55 K, 292.34K and 298.88K, K was seen for cells when simulated with 0.3C ,1C and 3 C rate respectively.

6.1.3 For single cell (water cooled) under different discharge rates:

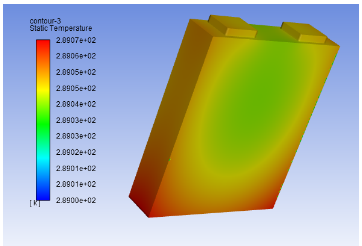

(a) At 0.3 C rate

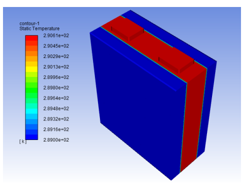

(b) At 1 C rate

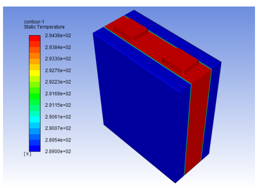

(c) At 3 C rate

Figure 6: Temperature contour of water-cooled cell

When the cell is simulated at a c-rate of 0.3, we can see that the heat generated on the cell when it is cooled by a stream of water at 0.5m/s, 289K causes the temperature to rise to about 289.07K. As the discharge rate increases, maximum temperature of cell is seen to be 290.61 and 294.38K at 1C and 3C discharge rate respectively. The effect of cooling on the cell can be seen across the cooling channel. The minimum temperature that occurs across the surface is 289K.

6.1.4 For single cell (cooled with 3M Novec 7100) under different discharge rates:

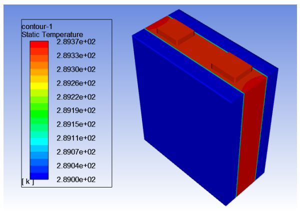

(a) At 0.3 C rate

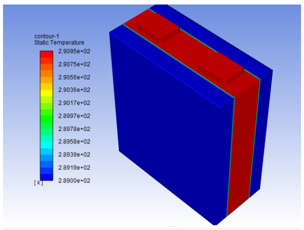

(b) At 1 C rate

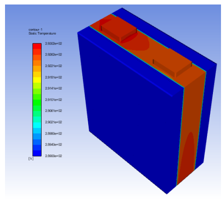

(c) At 3 C rate

Figure 7: Temperature of 3M- Novec cooled cell

As seen earlier, with increase in C-rate the temperature contours show increase in the cell temperature. The maximum temperature of the cell increased from 289.37 K at 0.3 C to 293.03 K at 3C respectively.

The variation in maximum and minimum temperature of the cell is shown in Table 3.

Table 3: Temperature variation for battery under different discharge cycle and coolants

S.N.	Coolant	Discharge rate	Maximum Temperature (K)	Minimum Temperature (K)
1	-	0.3	303.35	300
	-	1	306.8K	300
	-	3	311.04	300
2	Air	0.3	290.55	289
	Air	1	292.344	289
	Air	3	298.88	289
3	Water	0.3	289.07	289
	Water	1	290.61K	289
	Water	3	294.38	289
4	3M Novec 7100	0.3	289.37K	289
	3M Novec 7100	1	290.95	289
	3M Novec 7100	3	293.03	289

From these figures and Table 3, we can observe that the maximum temperature of the cell when discharged is less for case 4, so we can say that the cooling effect produced by 3M Novec 7100 is the best.

6.2 For single cell under charge/discharge cycle

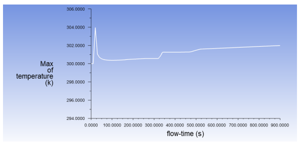

(a) Maximum temperature plot

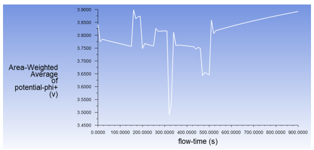

(b) Positive potential plot

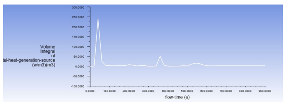

(c) Heat plot

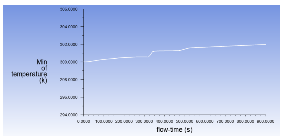

(d) Minimum temperature plot

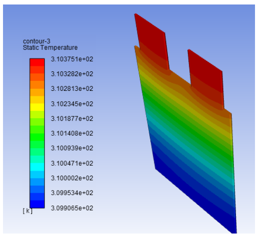

(e) Temperature contour

Figure 8: For single cell under charge-discharge cycle

By reviewing the plots, it can be found that the maximum temperature increase occurred during the discharging of the cell at 200W C for 150s, i.e. the 1st component of our cycle. The maximum temperature is found to be 303.9 K. It can also be seen that the potential of the battery decreases during the discharge processes and increases during the charging processes. However the volume of heat generation across the cell increases during discharge and decreases during charging processes.

6.2.1 For single cell (air cooled) under charge/discharge cycle:

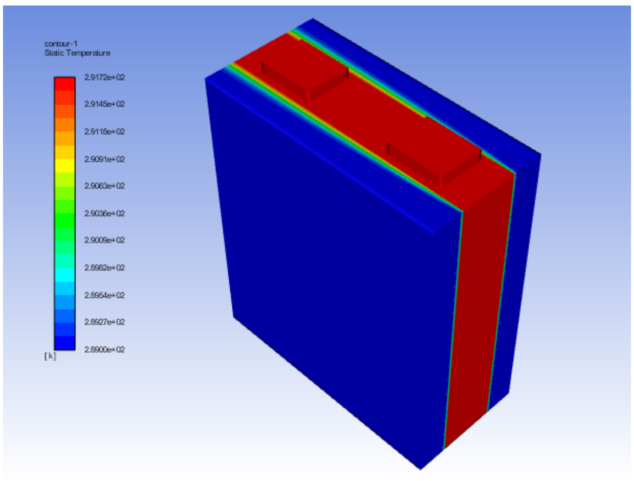

Figure 9: Temperature contour of cell under combination cycle cooled by air

From Figure 9 we can see that an air-cooled cell with air flowing at 0.5 m/s sets the minimum temperature at 289K and the maximum temperature that the cell can reach during the cycle is 291.7459 K.

6.2.2 For single cell (cooled by water) under charge/discharge cycle:

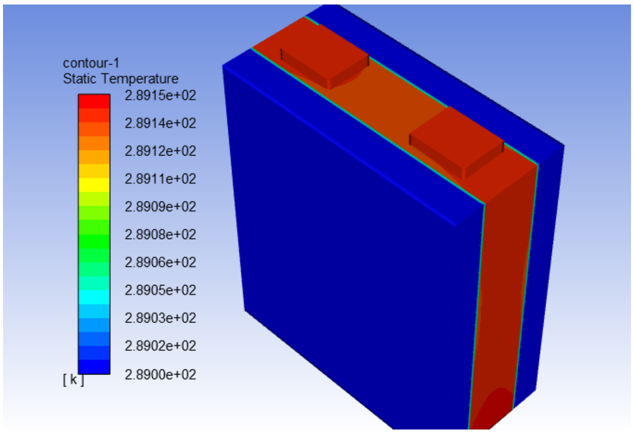

Figure 10: Temperature contour of cell under combination cycle cooled by water

From Figure 11,we can see that a water-cooled cell with water flowing at 0.5 m/s sets the minimum temperature at 289 K and the maximum temperature that the cell can reach during the cycle is 291.1782 K.

6.2.3 For single cell (cooled by 3M Novec) under charge/discharge cycle:

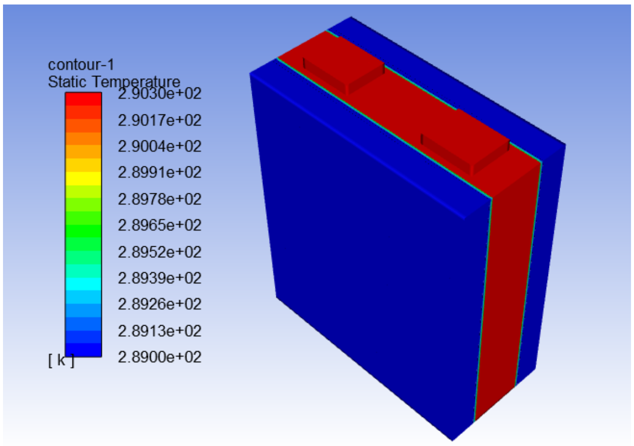

Figure 11: Temperature contour of cell under combination cycle cooled by 3M Novec-7100

From Figures 11, we can see that a 3M-Novec cooled cell with water flowing at 0.5 m/s sets the minimum temperature at 289 K and the maximum temperature that the cell can reach during the cycle is 291.2345 K. The results from the figures are summarized in Table 4.

Table 4: Temperature variation

SN.	Coolant	Max. Temperature	Min Temperature
1	-	303.9651 K	300 K
2	Air	291.7459 K	289 K
3	Water	291.1782 K	289 K
4	3M Novec	291.2359 K	289 K

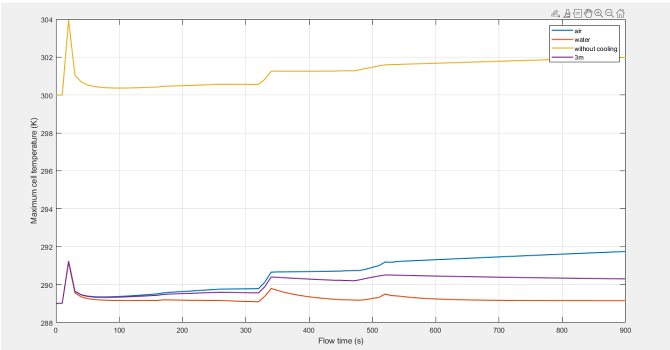

Figure 12: Temperature comparison plot for single cell with or without coolant

From this, we can find that the cooling effect of water was better during the charge/discharge cycle. Also, the use of air water, and 3M Novec 7100 brought the temperature of the cell down by 4.02%, 4.206%, and 4.18% respectively. The use of these coolants sets the minimum temperature of the cell to 289 K.

7. Experimental works

The experimental setup consisted of electrical and electronic systems to charge and perform discharge operations of the battery. The electrical and electronic system consisted of the power switch, a laptop (with EB tester software installed), electric connectors, a charger, an electric load (discharger), and several electrical connectors. An infrared contactless thermometer was used to measure the temperature of the battery during discharging applications. The module cell was charged to a 100% before the start of the experiment.

Figure 13: Experimental setup

7.1 Results

A Highstar 50Ah battery cell was discharged at a 0.3C discharge rate, and the measurement results were compared with the CFD thermal simulation of the cell at identical operating conditions. This testing was done at a temperature of 23 °C. The test value for current was 15A (0.3C). The results obtained from the simulation can be presented in two different ways. The first result included the temperature of the battery as the discharge process was conducted. The next result that was obtained was the plot for voltage and current with time as the discharge process took place, which was obtained automatically from the EBtester software. For this result, the input values were that of time, current to be released, and cutoff voltage from the battery.

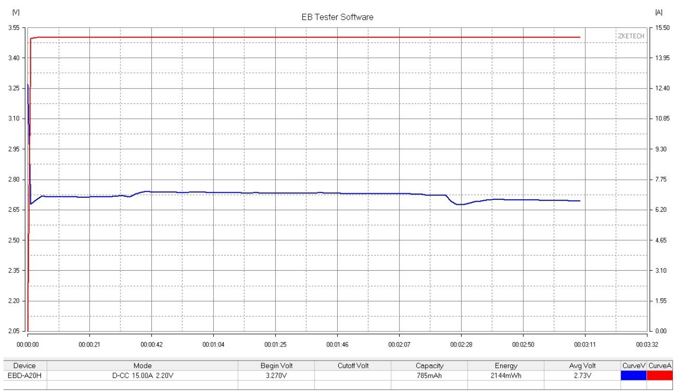

Figure 14: Results shown by EB tester software

The temperature of the cell on discharge was observed and the values at different time instances were noted.

The values obtained from test at 23°C and from simulation in ANSYS were compared and it was found that the values were closely similar. The values obtained from simulation were in close agreement with the experimental values.

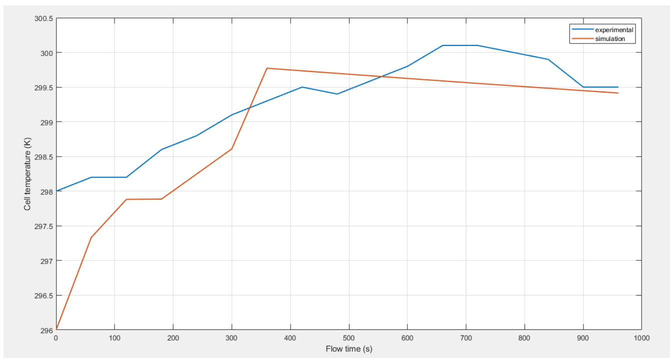

Figure 15: Comparison between experimental and simulation data

Also, the plot for temperature contour was obtained by simulation in ANSYS and is displayed in Figure 14. The cell appears to be heated in the tabs and it is slowly transmitted across the center of the cell.

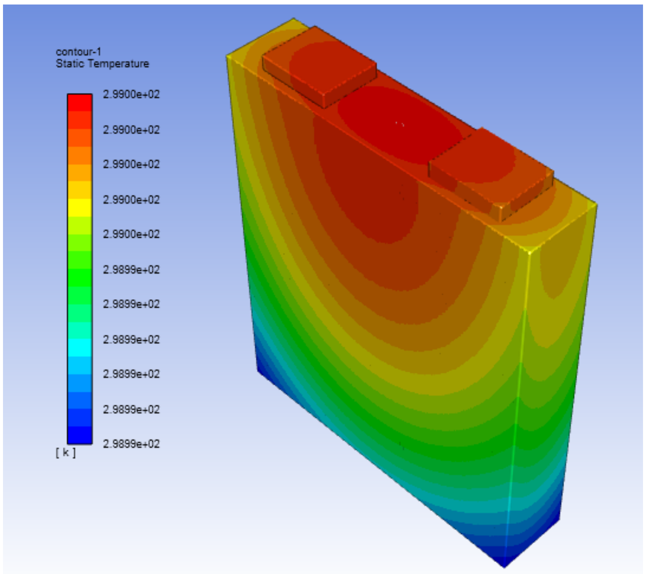

Figure 16: temperature contour of cell at 0.3 C-rate at 23 degree celsius

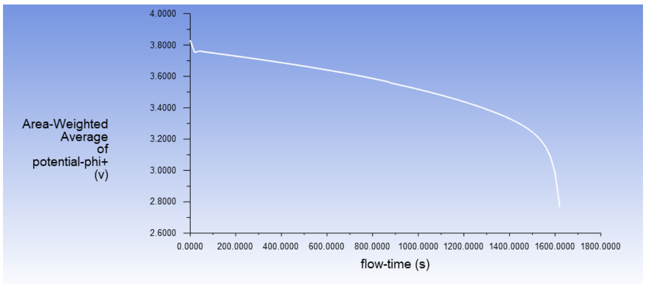

Figure 17: Potential plot obtained by simulation

From these plots, the dip in positive potential (phi+) can be easily observed in the discharging process. This was the plot obtained for the change in potential in the 0.3 C discharge rate of the battery. This curve is similar to the one we found in ANSYS simulation.

8. Conclusion

It was found that on increasing the discharge rate, the maximum temperature of the cell increased. The effect of different coolants on the maximum temperature of the cell was observed and it was found that among the three different coolants used, 3M Novec-7100 proved to the best coolant for simple discharge conditions. Meanwhile, when the cells were simulated according to a combined cycle, water proved to be the best coolant for both cases.

Acknowledgments

The authors are thankful for the support provided by the staff in the Department of Mechanical and Aerospace Engineering at IOE, Pulchowk Campus.

References

[1] Fiorentino Valerio Conte. Battery and battery management for hybrid electric vehicles: a review. *e & i Elektrotechnik und Informationstechnik*, 123(10):424–431, 2006.

[2] Ahmad Pesaran, S Santhanagopalan, and GH Kim. Addressing the impact of temperature extremes on large format li-ion batteries for vehicle applications (presentation). Technical report, National Renewable Energy Lab.(NREL), Golden, CO (United States), 2013.

[3] Chester G Motloch, Jon P Christophersen, Jeffrey R Belt, Randy B Wright, Gary L Hunt, Raymond A Sutula, Tien Duong, Thomas J Tartamella, Harold J Haskins, and Ted J Miller. High-power battery testing procedures and analytical methodologies for hev's. *SAE Transactions*, pages 797–802, 2002.

[4] Jie Sun, Jigang Li, Tian Zhou, Kai Yang, Shouping Wei, Na Tang, Nannan Dang, Hong Li, Xinping Qiu, and Liquan Chen. Toxicity, a serious concern of thermal runaway from commercial li-ion battery. *Nano Energy*, 27:313–319, 2016.

[5] Ahmad A Pesaran. Battery thermal models for hybrid vehicle simulations. *Journal of power sources*, 110(2):377–382, 2002.

[6] Jaewan Kim, Jinwoo Oh, and Hoseong Lee. Review on battery thermal management system for electric vehicles. *Applied thermal engineering*, 149:192–212, 2019.

[7] Abubakar Gambo Mohammed, Karem Elsayed Elfeky, and Qiuwang Wang. Recent advancement and enhanced battery performance using phase change materials based hybrid battery thermal management for electric vehicles. *Renewable and Sustainable Energy Reviews*, 154:111759, 2022.

[8] Rhodri E Owen, James B Robinson, Julia S Weaving, Martin TM Pham, Thomas G Tranter, Tobias P Neville, Duncan Billson, Michele Braglia, Richard Stocker, Annika Ahlberg Tidblad, et al. Operando ultrasonic monitoring of lithium-ion battery temperature and behaviour at different cycling rates and under drive cycle conditions. *Journal of The Electrochemical Society*, 169(4):040563, 2022.

[9] Huaqiang Liu, Zhongbao Wei, Weidong He, and Jiyun Zhao. Thermal issues about li-ion batteries and recent progress in battery thermal management systems: A review. *Energy conversion and management*, 150:304–330, 2017.

[10] Ahmet AKTÜRK, Melih YILDIZ, and Mehmet Emin ARICI. Temperature variation of a li-ion battery module operated at the driving cycle for different cooling rates. *The 5th International Conference on Alternative Fuels, Energy & Environment: Future and Challenges*, 2021.

[11] Petr Vyroubal, Tomás Kazda, Jiří Maxa, and Jirí Vondrák. Analysis of temperature field in lithium ion battery by discharging. *ECS Transactions*, 70(1):269, 2015.

[12] MS Windows NT Battery pack & configuration. Available at `https://evkx.net/technology/battery/batterypack/?fbclid=IwAR3BNHIJS66YydGsPlxpgSSZQE4E4My_P27RB7HzxK2M2Yr3pxMb0oI_ixg` Accessed on: (2023/08/05).